

mouse IgG, PE-Cy5 labeled mouse IgG1 and PE labeled mouse IgG1.

Results: Endothelial microparticles were significantly elevated in patients with HNC patients (CD31+/CD62E+/CD42b-: mean  $1601 \pm 1479$  EMP/ $\mu$ l; CD31+/CD142+/CD42b-: mean  $121 \pm 135$  EMP/ $\mu$ l) compared with control group (CD31+/CD62E+/CD42b-: mean  $782 \pm 698$  EMP/ $\mu$ l; CD31+/CD142+/CD42b-: mean  $688 \pm 647$  EMP/ $\mu$ l). The concentration of EMP were not notably increased as result of RT/RCT (CD31+/CD62E+/CD42b-: mean  $1629 \pm 769$  EMP/ $\mu$ l; CD31+/CD142+/CD42b-: mean  $1257 \pm 603$  EMP/ $\mu$ l). There were no significant differences between EMP level before treatment, one day and 3 months after radiation cessation. Furthermore, there was no significant difference in plasma EMP level in plasma of the HNC patient undergoing RT alone, RT combined with chemotherapy, postoperative RT or postoperative RCT.

Conclusions: The data suggest that the release of EMP is not a marker of ECs activation as a result of early response to ionizing radiation during RT/RCT in HNC patients.

---

Poster: Radiobiology track: Predictive assays/prognostic factors

---

#### PO-1076

Unsupervised clustering in gene expression profiling to make prognosis for malignant gliomas

B. Yang<sup>1</sup>, W.W. Lam<sup>1</sup>, K.Y. Cheung<sup>1</sup>, S.K. Yu<sup>1</sup>

<sup>1</sup>Hong Kong Sanatorium & Hospital, Medical Physics and Research Department, Happy Valley, Hong Kong (SAR) China

Purpose/Objective: Prediction of the treatment response and overall outcome in patients is an important goal in radiation oncology. We aim to identify prognostic molecular features using gene expression profiling in gliomas.

Materials and Methods: Data from [1] were used in this study. Total 152 samples including 100 glioblastomas, 21 anaplastic astrocytomas, 19 diffuse astrocytomas and 12 anaplastic oligodendrogliomas were selected for analysis and 3456 genes expressed in gliomas, including 3012 unique sequences plus an additional 444 genes from a literature survey were identified. Different from using a selected training set in [1], the total 152 samples were included in our study. Progression-free survival (PFS) period was adopted as the clinical parameter for the treatment response. Pearson's linear correlation coefficients between the gene data and PFS record were computed for selecting the candidate genes for prognosis model. Hierarchical clustering was then computed based on the expression profile of selected genes. Cox proportional hazards regression was used to calculate the hazard ratios between different groups.

Results: 47 genes are selected for our prognosis model and we have 29 genes in common with results in [1]. The unsupervised hierarchical clustering allows us to cluster the 152 patients into three distinct groups based on their similarities measured over those selected 47 genes. The results of Kaplan-Meier analysis for all patients show PFS probabilities after 5 years are 70.2%, 0% and 25.7% for group 1, 2 and 3 respectively. The cox proportional hazards regression analyses show hazard ratios 23.0, 8.8 and 0.6 for

group 1&2, group 1&3 and group 2&3 respectively. The same method is also applied on the non-glioblastoma patients, which are able to be clustered into two groups with PFS probabilities after 5 years 76.0% and 0% for group 1 and 2 respectively. The hazard ratio is calculated to be 25.5.

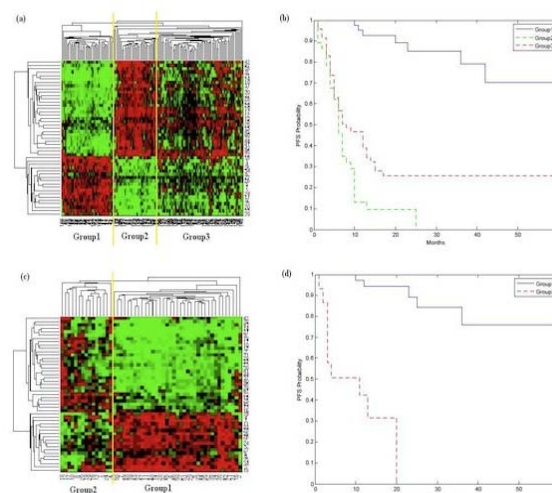


Fig. 1 (a) (b) Heatmap and Kaplan Meier plot for all patients; (c) (d) Heatmap and Kaplan Meier plot for non-glioblastoma patients.

Conclusions: In our analyses, the selected profiling results are useful in constructing a classification scheme and the unsupervised clustering method also succeeds in dividing the samples into good and poor prognosis groups. Compared with the results in [1], the good prognosis group in our result has higher PFS probabilities after 5 years and the unsupervised method is direct and easy to prevent the possible bias in the selection of training set in the supervised method. [1] M. Shirahata, S. Oba, K. Iwao-Koizumi, S. Saito, N. Ueno, M. Oda, N. Hashimoto, S. Ishii, J. A. Takahashi and K. Kato, *Cancer Sci*, 100: 165-172

---

Poster: Radiobiology track: Others

---

#### PO-1077

Comparison of in vivo and theoretical assessment of radiation-induced DNA damage

M. Ebert<sup>1</sup>, B. Dahl<sup>2</sup>, J. Prunster<sup>2</sup>, N. Zeps<sup>3</sup>, B. Reniers<sup>4</sup>, F. Verhaegen<sup>5</sup>, C. Saunders<sup>6</sup>, M. House<sup>2</sup>, D. Joseph<sup>7</sup>

<sup>1</sup>Sir Charles Gairdner Hospital, Academic Physics, Perth Western Australia, Australia

<sup>2</sup>University of Western Australia, Physics, Perth Western Australia, Australia

<sup>3</sup>St John of God Hospital, Pathology, Subiaco Western Australia, Australia

<sup>4</sup>Maastric Clinic, Medical Physics, Maastricht, The Netherlands

<sup>5</sup>Maastric Clinic, Radiotherapy Physics, Maastricht, The Netherlands

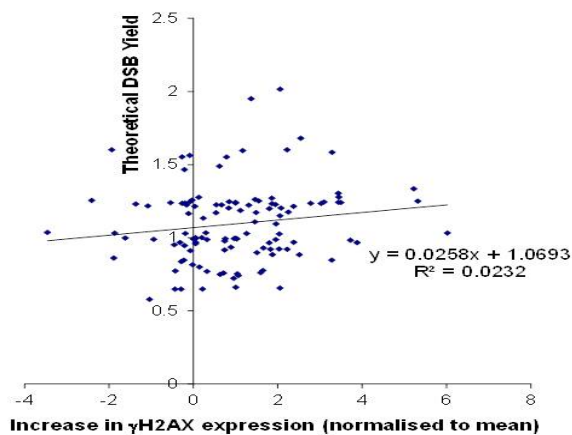
<sup>6</sup>University of Western Australia, Surgery, Perth Western Australia, Australia

<sup>7</sup>Sir Charles Gairdner Hospital, Radiation Oncology, Perth Western Australia, Australia

**Purpose/Objective:** Comparison of theoretical estimation of lethal DNA damage of normal mammalian cells during exposure to low-kV X-rays with an ex vivo assessment of double-strand strand breaks (DSBs) in tissue irradiated in vivo.

**Materials and Methods:** 130 patients were treated with Intrabeam intraoperative radiotherapy of the tumour bed following breast cancer resection. Tissue samples were taken from the resection wall before and after irradiation with 50 kV X-rays. Doses of 5 to 6 Gy were delivered at 1 cm from the edge of a treatment applicator. Time for dose delivery varied between 10 and 40 minutes. Tissue samples were sectioned and stained for phosphorylated  $\gamma$ H2Ax, representative of DNA repair, to assess damage before and after irradiation. The proportion of stain was recorded on multiple slides spanning samples from 130 patients. Monte Carlo radiation transport calculations were used to determine the spectra of secondary electrons at the samples in situ. These spectra were used as input to a damage simulation code producing expected levels of damage. In combination with expected repair rates and irradiation times, theoretical estimates of DSBs remaining at the end of irradiation were made based on the linear-quadratic model of radiation damage with repair.

**Results:** Considerable variability was found in change in  $\gamma$ H2Ax expression between pre and post-irradiation sections, though there is a trend for decreased accumulation with longer irradiation time, consistent with increased proportional repair. The theoretical results suggest a reduction in damage with increasing applicator size due to both increased beam hardening and longer irradiation times. There is however little similarity between theoretical and experimental determination of induced DSBs, with poor correlation as shown in the figure.



**Conclusions:** Assessment of DNA damage occurring in humans is difficult and rare. We found poor correlation between theoretical DSB estimates and those made using ex vivo assessment of tissue samples. It is likely that insufficient time was available post irradiation for accumulation and equilibrium of  $\gamma$ H2Ax. With potentially slow repair and a diversity of cell types present in sections, larger numbers of patients may allow differences in in vivo normal tissue repair with dose-rate to be distinguished above levels of noise and uncertainty in both the measurements and the model.

PO-1078

Ionizing radiations sustain Glioblastoma cell dedifferentiation to a stem phenotype through Survivin  
 P. Dahan<sup>1</sup>, J. Martinez Gala<sup>1</sup>, C. Delmas<sup>1</sup>, S. Monferran<sup>2</sup>, L. Malric<sup>1</sup>, D. Zentkowski<sup>1</sup>, V. Lubrano<sup>3</sup>, C. Toulas<sup>1</sup>, E. Cohen-Jonathan Moyal<sup>1</sup>, A. Lemarié<sup>1</sup>

<sup>1</sup>INSERM U1037 CRCT, Experimental Therapeutics, Toulouse, France

<sup>2</sup>INSERM U1037 CRCT, Molecular & Cellular Oncology, Toulouse, France

<sup>3</sup>INSERM U825, Neurosurgery, Toulouse, France

**Purpose/Objective:** Glioblastomas (GBM) are some highly lethal brain tumors despite a conventional treatment associating surgical resection and subsequent radio-chemotherapy. Amongst these heterogeneous tumors, a subpopulation of chemo- and radioresistant GBM stem-like cells appears to be involved in the systematic GBM recurrence. Moreover, recent studies showed that differentiated tumor cells may have the ability to dedifferentiate and acquire a stem-like phenotype, a phenomenon also called plasticity, in response to microenvironment stresses such as hypoxia. We hypothesized that GBM cells could be subjected to a similar dedifferentiation process after ionizing radiations (IR), then supporting the GBM rapid recurrence after radiotherapy.

**Materials and Methods:** In the present study we established several differentiated GBM cell lines isolated from patient resections and subjected them to a clinically relevant IR dose (3 Gy). We then characterized, after long term culture, the phenotypic and functional alterations displayed by these GBM cells using *in vitro* techniques (qPCR, western blot, flow cytometry, limiting dilution clonogenic assays) and *in vivo* experiments (orthotopically-xenografted nude mice).

**Results:** We demonstrated that the exposure of differentiated GBM cells to a subtoxic IR dose potentiated the long-term reacquisition of stem-associated properties such as the ability to generate primary and secondary neurospheres, the expression of stemness markers and an increased tumorigenicity. We also identified during this process an up-regulation of the anti-apoptotic protein survivin and we showed that its down-regulation by YM-155, a selective survivin inhibitor used in anti-cancer clinical trials, led to the blockade of the IR-induced plasticity.

**Conclusions:** Altogether, these results demonstrated that irradiation could regulate GBM cell dedifferentiation via a survivin-dependent pathway. Targeting the mechanisms associated with IR-induced plasticity will likely contribute to develop some innovating pharmacological strategies for an improved radiosensitization of these aggressive brain cancers.

PO-1079

Single W18049 nanowire: a multifunctional nanoplatform for image-guided dose-enhancement radiation therapy  
 Q. Xiao<sup>1</sup>, W. Bu<sup>1</sup>, Y. Ren<sup>2</sup>, J. Qiu<sup>2</sup>, Z. Xiangpeng<sup>2</sup>

<sup>1</sup>Shanghai Institute of Ceramics Chinese Academy of Sciences, State Key Laboratory of High performance Ceramics and